Flame Kernel Formation in a Spark-Ignition Engine

R.Herweg and G.F.W.Ziegler

Institut für Physikalische Elektronik
Universität Stuttgart
Pfaffenwaldring 47
D-7000 Stuttgart 80
F.R.Germany

ABSTRACT

The effects of mixture turbulence on flame kernel formation in a spark-ignition engine were investigated by using a disc-shaped optically accessible combustion chamber.

The flow field was investigated by LDA. High-speed schlieren films up to 40 kHz were taken simultaneously from two orthogonal directions to visualize the formation and development of the flame kernel in detail. The purpose was to gain a better understanding of the interaction of the turbulence and the flame during the first milliseconds after spark onset up to a flame diameter of 10 mm.

Image processing was performed to determine the schlieren contour of every single frame.

This study shows that the flame kernel shape is changed by the turbulence at flame radii of 0.5 to 1 mm depending on turbulence intensity. At flame radii of more than 10 mm a fully developed turbulent flame has been formed. The influence of turbulence on the turbulent burning velocity during the flame kernel formation is less than during the main combustion period.

INTRODUCTION

Flame kernel formation in an internal combustion engine begins with the spark onset and terminates when a developed flame of about 10 mm is attained. The objective of this study was to determine the flame propagation in this very early stage of combustion. Flame kernel formation depends on the mixture composition, thermodynamic state, fluid motion, ignition system and spark plug design.

An effective way to study the structure and development of the early flame is the use of visualization techniques, since the pressure signal cannot resolve the period of flame kernel formation. In the direct photography studies of engine combustion optical access has been obtained either through the cylinder head or the piston with a single window [1], [2]. [1]

Schlieren photography or shadowgraphy have used a quartz cylinder head and a mirror on the piston [3], [4] or a quartz piston and a mirrored cylinder head [5]. Another approach to get optical access is to apply a square piston engine with quartz walls [6], [7], [8].

There are still different opinions existing concerning the structure and the propagation process of flame kernels. Chomiak [9] describes the flame kernel formation being independent of flow mixture velocity and composition. Namazian et al. [6] and Smith [10] detect irregularities within the flame kernel once it fills the electrode gap, whereas Bradley and Lung [11] do not observe any turbulence interactions within the first 0.2 ms. Keck et al. [12] and Tagalien and Heywood [13] show a laminar like burning process immediately following the spark discharge and an expansion speed of the flame kernel which increases approximately linearly with the burned gas radius. They point out that the most important parameters controlling the initial flame growth are the laminar burning velocity and the size of the first eddy burned. ZurLoye [14] showed that the flame kernel is influenced by the turbulence 0.1 ms after spark onset by using a laser light sheet measuring technique.

This work has been performed in a disc-shaped combustion chamber, where optical access from two directions is feasible. The initial flame growth process is examined under a variety of conditions of mixture composition, engine load, spark gap distance and engine speed.

EXPERIMENTAL SET-UP

Figure 1 shows a schematic of the test engine used in this study. It is possible to visualize the flame kernel region from two orthogonal directions. Encluded are the positions for the LDA-measurements in this combustion chamber.

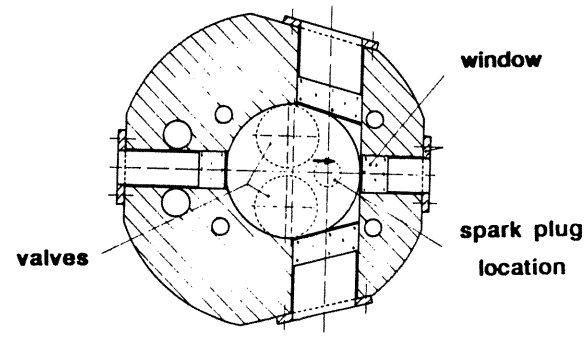

Figure 1: Disc chamber with orthogonal view.
Bore 73 mm, stroke 67 mm, compression ratio 7.3

A pressure transducer in the combustion chamber measured pressure traces during engine operation. A piezo-resistive transducer in the inlet port system determined the inlet pressure at inlet valve closing point. A transistorized coil ignition system (TCI) was applied.

Accurate control of the engine and synchronization of recorded data was achieved by an electronic control unit (Fig. 2). This device controlled the data aquisition system, the two rotating mirror cameras, the spark flash light source, the ignition timing, and the charge control. The unit was driven by input signals from a crank angle mounted shaft encoder delivering signals every half crank angle degree. An electrical motor was used to control the engine

[1] Numbers in parenthese designate references at end of paper

speed. The engine was preheated and operated in a skipped-fired mode to eliminate residual gas. Therefore a constant propane-air mixture was flowing through the combustion chamber, while motoring the engine at the determined engine speed. The air and propane flow rates were monitored by a Brooks mass flow meter and mass flow controller with an accuracy of 1%. Mixing of both was performed via a Venturi nozzle and a special mixing tank to reduce pumping effects in the inlet system.

Figure 3 gives a schematic representation of the high-speed schlieren photography. A purpose-built spark flash light source is used to illuminate the combustion chamber from two orthogonal directions with a frequency up to 40 kHz and a pulse duration of 20 ns. For each direction, a schlieren system built of condenser, schlieren lens, circular schlieren stop and camera optics is set up. Two rotating mirror cameras are used to get the pictures with a negative size of 20 mm. Image processing is performed after negative processing to determine the schlieren contour of every single frame.

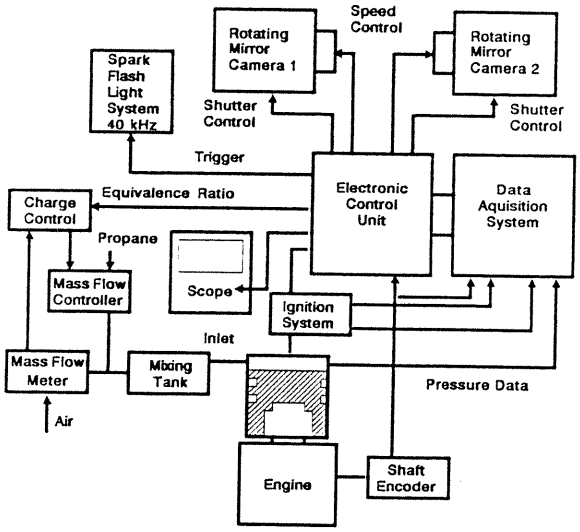

Figure 2: Electronic Instrumentation

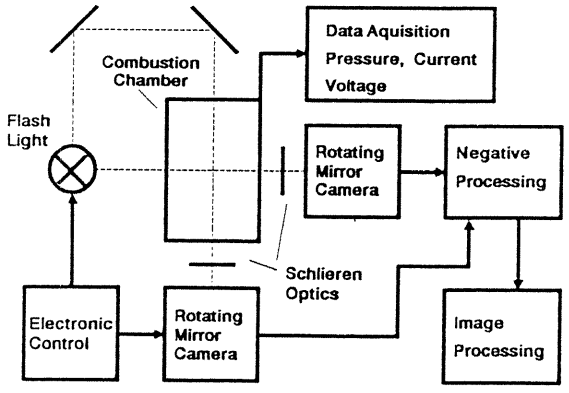

Figure 3: Schematics of high-speed schlieren photography

LDA MEASUREMENTS

Flow velocities have been determined in axial and radial directions at different points near the spark plug with a resolution of 1 crank angle (Fig. 1). Cyclic variations on the signal were extracted from the averaged signal by the procedure described in [15]. Mean velocity and turbulence intensity are scaled linearly with engine speed, which can be seen after the normalization to the mean piston speed. Fig. 4 shows the cycle-resolved values for the mean flow velocity and turbulence intensity.

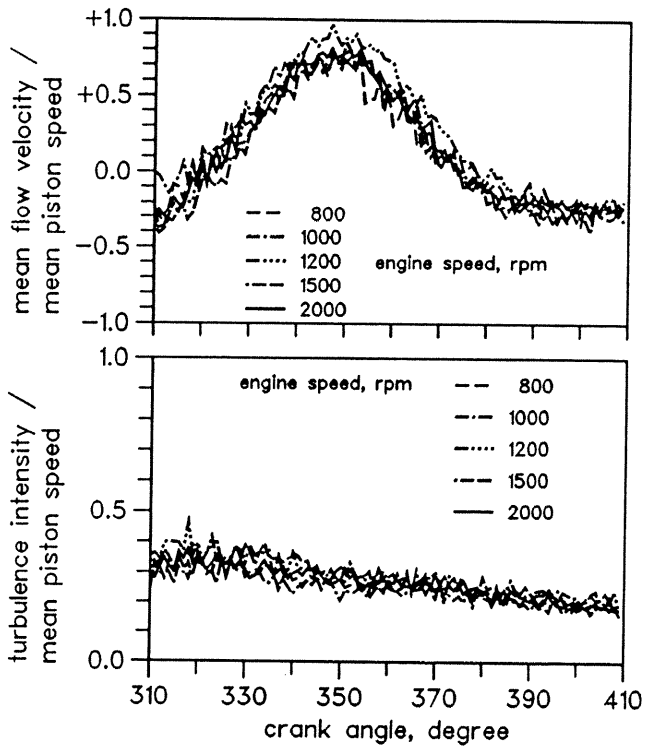

Figure 4: LDA measurements of mean flow velocity and turbulence intensity versus crank angle in radial direction

TEST CONDITIONS

The test conditions for the present study are given in Table 1. It is important mentioning that during all experiments the ignition timing is kept constant at 330 CAD, even while the air-fuel ratio, the load and the engine speed are changed. This was done to keep the flow field structure at ignition timing constant. Therefore a nearly constant temperature and pressure results at spark onset. No MBT [3] ignition timing was used since the main purpose was to investigate the flame kernel formation at well-defined and comparable conditions. For changing the air-fuel ratio the airstream was fixed and the fuel was controlled by the mass flow controller, resulting in an air-fuel ratio within 1% accuracy. The conventional transistorized-coil ignition system (TCI) provided a maximum electrical energy of 50 mJ to the coil with a spark duration of some milliseconds, depending on engine speed. For all conditions six single high resolved cycles have been recorded. Additionally 45 cycles at constant crank angles, which were changed consequently with a constant interval until the flame had lost the window area have been picked up, to give the mean volume and its standard deviation at different crank angles.

Table 1: Test Conditions

Engine speed (rpm)	800, 1000, 1200, 1500, 2000
Normalized air-fuel ratio	1.0, 1.3
Residual mass fraction	0
Ignition timing (CAD)[2]	330
Mixture inlet temperature (K)	298
Pressure at ignition timing (bar)	part load, full load
spark gap distance (mm)	0.7, 1.0, 1.2
Fuel	propane
Ignition system	TCI

[2]crank angle degree
[3]maximum brake torque

RESULTS FROM HIGH-SPEED SCHLIEREN PHOTOGRAPHY

Figure 5 shows both optical views of the flame kernel at a definite time after spark onset as an example for the high-speed schlieren pictures. Increasing engine speed leads to a faster development of the flame kernel, because mainly turbulence intensity is changed. The increasing turbulence intensity can be seen in the inner core and at the outline of the kernel, where the decreasing length scales are wrinkling the surface of the flame.

Figure 6 shows the developing turbulent flame in the disc chamber. Only one direction is given here. Between the spark gap the flame kernel shows a laminar like behaviour. But soon after leaving the spark gap region it will be influenced by the surrounding flow field. This is normally independent of the air-fuel ratio, which will increase the time interval to reach a flame radius of about 1 mm, at which wrinkling appears. This longer time duration is caused by the decreasing laminar burning velocity with increasing air-fuel ratio.

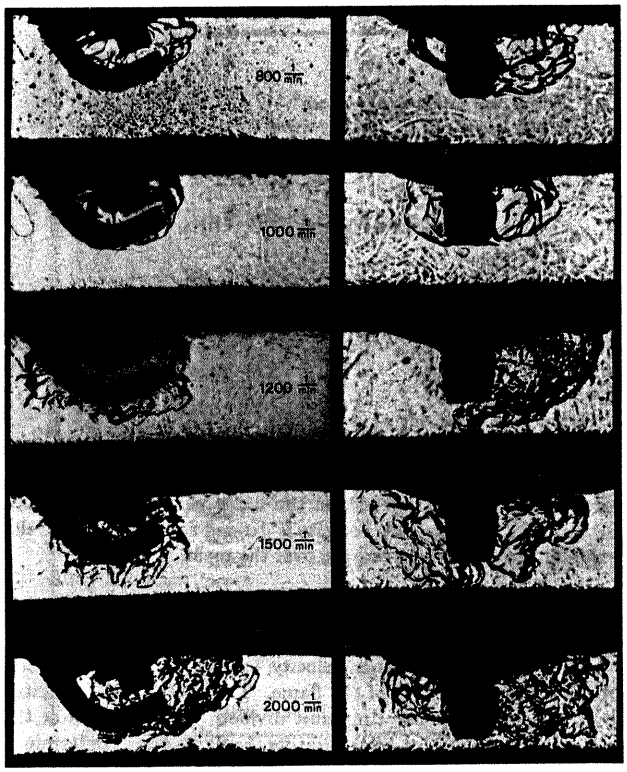

Figure 5: Schlieren frames at different engine speed 1.1 ms after spark onset, TCI, ignition timing 330 CAD, part load, normalized air-fuel ratio 1.0.

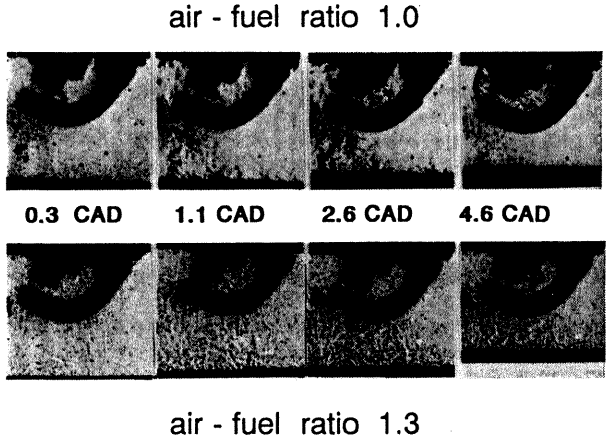

Figure 6: Schlieren sequences in the disc chamber (crank angles referring to spark onset), 800 rpm, TCI, ignition timing 330 CAD, part load.

ANALYSIS OF THE FLAME KERNEL FORMATION

For analyzing the schlieren pictures the single frames were digitized by an image processing system. The resulting contours of the two different orthogonal projections of the burned area were taken to calculate the burned volume. Therefore the third orthogonal projection was built with the assumption that the single points of the measured boundary are describing the axis of an ellipse. By integrating the resulting elliptical discs one can get the enflamed volume and the surface of an alternative body of the flame kernel. A further assumption is that all the gas inside this enflamed volume is burned and no unburned islands exist behind the flame front. This is also shown by Beretta et al.[2] and Gatowski and Heywood [16], who determined, that the difference between the burned gas radius and the flame radius is small during the early development of the flame. This suggests that entrainment of unburned gas behind the flame front is small. For the given parameters the flame front thickness is about 0.1 mm [3]. Modern flamelet theories separate consequently between burned and unburned regions [17], [18]. Figure 7 gives an example of the evolution of the enflamed volume for six single high resolved cycles and the result from 45 cycles at different crank angles for statistical analysis.

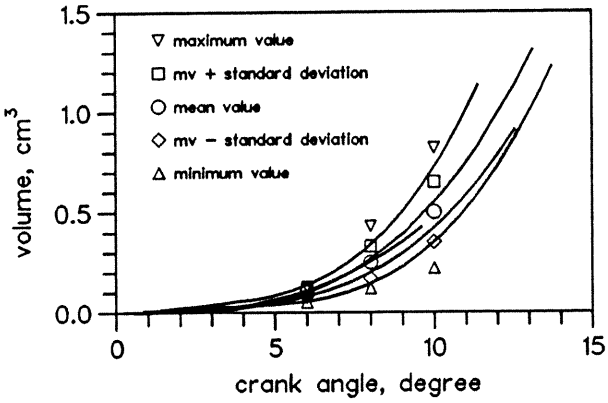

Figure 7: Example of the volume evolution of six single cycles and the results from statistical analysis. 1500 rpm, TCI, ignition timing 330 CAD, full load.

To compress the data of the flame kernel evolution the next figures show the crank angle interval after spark onset to reach an enflamed volume of 0.1 cm^3, 0.2 cm^3, 0.3 cm^3, 0.4 cm^3 and 0.5 cm^3.

Figure 8 shows the evolution of the enflamed volume at different engine speeds and different normalized air-fuel ratios in the disc chamber. With higher engine speed the time interval to reach the same volume is decreasing. All points are calculated from the 45 different cycles to find a mean value and its standard deviation. With higher air-fuel ratios and therefore lower burning velocities the time interval is also decreasing till the same volume is enflamed.

Figure 9 shows the evolution of the enflamed volume, while the spark gap distance is changed. The increasing spark gap leads to a faster flame kernel development. The minimum ignition energy for the mixture is reduced because of the reduced heat losses to the electrodes [19]. With increasing air-fuel ratio the evolution is also decreasing, but because of the lower laminar burning velocity.

Load was changed in the range of 4 to 7 bar at 330 CAD. There is no difference, when laod is increased (Fig. 10). The main reason is the dominant influence of the laminar burning velocity [20], which is more sensitive to temperature than to pressure changes. Because of the constant ignition timing there is no change in temperature. The same influence up to a mass burn rate of 1% was found by Csallner [21].

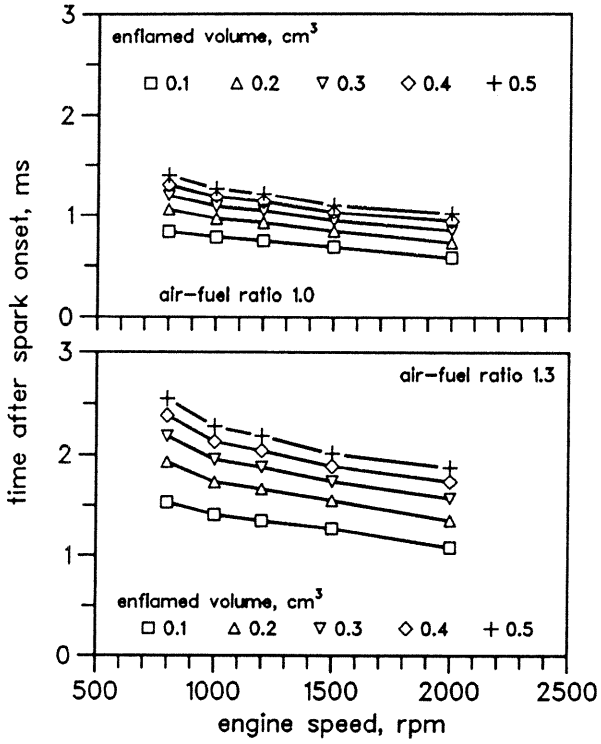

Figure 8: Enflamed volume evolution at different engine-speeds and different normalized air-fuel ratios, TCI, ignition timing 330 CAD, part load.

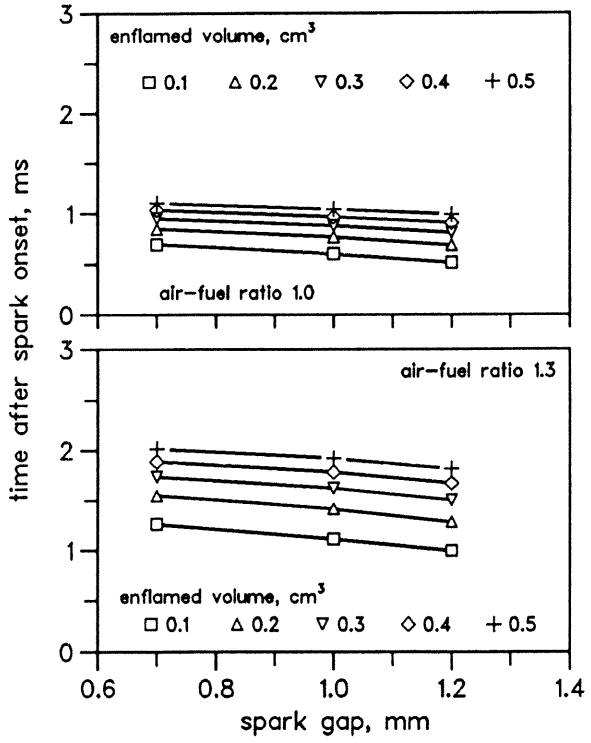

Figure 9: Enflamed volume evolution at different spark gap distances and different normalized air-fuel ratios, 1500 rpm, TCI, ignition timing 330 CAD, part load.

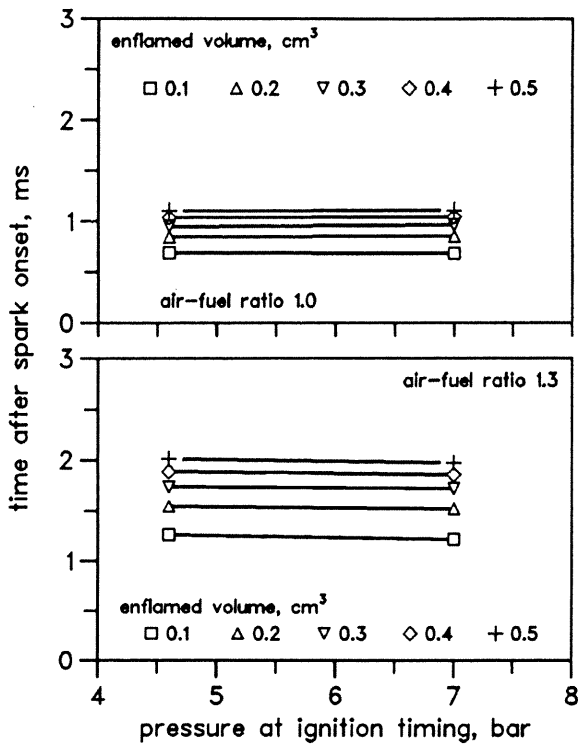

Figure 10: Enflamed volume evolution at different engine-load and different normalized air-fuel ratios, 1500 rpm, TCI, ignition timing 330 CAD.

EXPANSION VELOCITIES

The mean flame front or expansion velocity has been calculated to recognize differences in the flame kernel formation and development period. This velocity is defined as the velocity of the expanding flame front averaged over the mean flame area.

$$v_f = \frac{\dot{V}_b}{A_f} \tag{1}$$

where v_f is the expansion velocity, V_b is the burned volume and A_f is the mean surface of the flame. This velocity is calculated by the volume rise per time unit divided by the surface of the enflamed volume or by differentiating the flame radius determined from the enflamed volume and the surface.

Examples of the flame radius and the expansion velocity are depicted in Fig.11 and 12. Generally after spark breakdown the expansion velocity drops within 0.5 ms. This is caused by the initially fast expansion of the discharge channel which is due to the excess of spark energy compared to the minimum ignition energy [22]. After this period an initial level of the expansion velocity is attained, which is influenced by the air-fuel ratio, and the turbulence intensity. A similar tendency has been obtained by Pischinger and Heywood [23], Lancaster et al. [24] and Baritaud [25] for the flame development phase. For low engine speeds this initial level is very close to that of a laminar flame. Therefore the laminar chemistry, depending on the thermodynamic state and mixture composition, controls the flame kernel fomation. Increasing the engine speed and therefore the turbulence intensity, however, leads to an increase of this initial level expansion velocity due to wrinkling of the flame front. At flame radii of about 4 mm the expansion velocity is increasing to higher values.
Fig. 13 shows this tendency, where the expansion velocity is given versus the flame radius.

These expansion velocities can be compared to the laminar expansion velocity at the same pressure and unburned gas temperature. Since the pressure rise due to combustion can be neglected

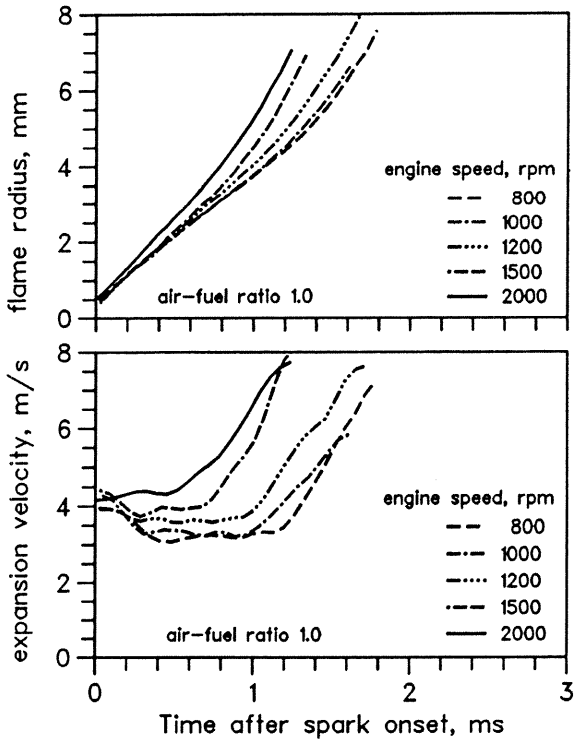

Figure 11: Flame radius and expansion velocity versus time, normalized air-fuel ratio 1.0, part load, spark gap distance 0.7 mm

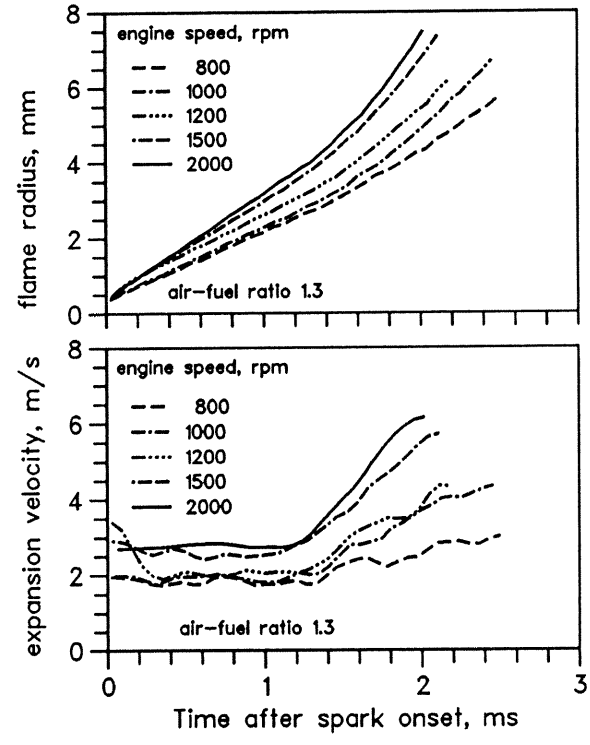

Figure 12: Flame radius and expansion velocity versus time, normalized air-fuel ratio 1.3, part load, spark gap distance 0.7 mm

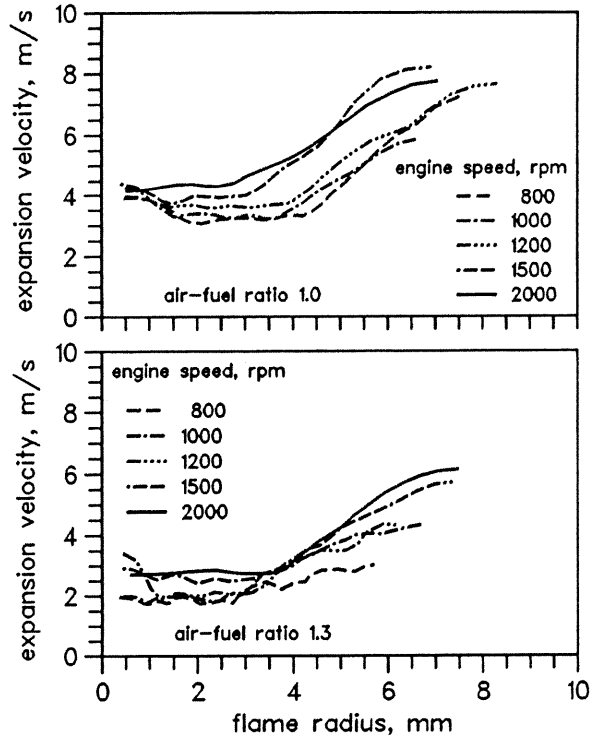

Figure 13: Expansion velocity versus flame radius, part load, spark gap distance 0.7 mm

during the flame kernel formation, it is possible to calculate with a constant density ratio between the unburned and the burned gas. The laminar burning velocity itself is a function of the pressure, the unburned gas temperature and the composition given by the air-fuel ratio and the residual gas fraction [20].
Then the laminar expansion velocity is determined by

$$v_l = \frac{\rho_u}{\rho_b} s_l \tag{2}$$

where v_l is the laminar expansion velocity and ρ_u and ρ_b are the densities of the unburned and burned mixture. Even for low engine speeds and turbulence levels the expansion velocity is higher than the laminar expansion velocity with the tendency to increase steadily with higher engine speeds and therefore higher turbulence intensities. This effect results from the basic mechanism which increases the burning velocity. Turbulence increases the burning velocity by wrinkling of the flame area. When the flame kernel is small, only small-scale eddies can provide this wrinkling: large-scale eddies convect the kernel without distorting it. As the flame kernel grows, the flame front can be wrinkled by increasing large eddies.

The ratio of the initial turbulent burning velocity, i.e. the expansion velocity divided by the unburned/ burned density ratio, to the laminar burning velocity, is plotted against the ratio of the turbulence intensity to the laminar burning velocity in Fig. 14. This demonstrates the turbulent formation and development of the flame kernel during the first milliseconds. This is a well known presentation for fully developed turbulent flames [14], but it is a convenient plot for the developing kernel, too. Of course this normalization does not include any effects of turbulence scales, which will have some influences, too. Also it is worth mentioning that the spectrum of the turbulence for the flame kernel is not the same as for fully developed flames, because only higher frequencies and therefore smaller scales can influence the flame kernel development [26]. All values for the normalization are taken from the LDA measurements, which give fully developded numbers. It is seen that with increasing engine speed, i.e. turbulence intensity, the turbulent burning velocity is increasing.

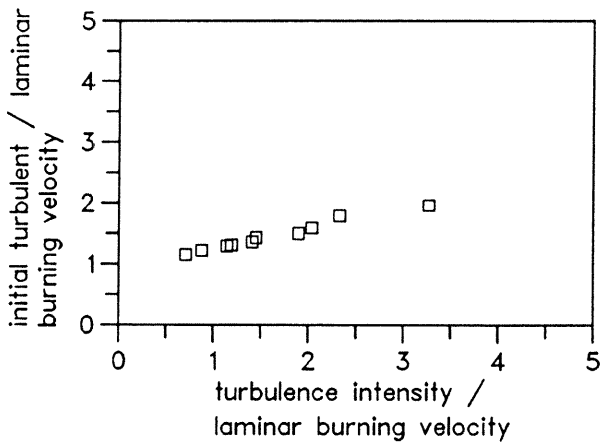

Figure 14: Normalized initial burning velocity versus normalized turbulence intensity, ignition timing 330 CAD, part load.

CONCLUSIONS

High speed schlieren photography in an optically accessible disc chamber shows that the expansion velocity drops within 0.5 ms from spark induced high values to an initial level, being characteristic of the flame kernel formation. This initial expansion velocity is very close to that of a laminar flame at low engine speeds or turbulence intensities. Therefore, the laminar flame chemistry, depending on the thermodynamic state and mixture composition, controls the flame kernel formation. Increasing the turbulence intensity, however, leads to a steady increase of this initial level expansion speed due to the wrinkling of the flame area. The turbulent burning velocity during flame kernel formation is considerably less than that of a fully developed flame. The flame kernel shape is changed by the turbulence at flame radii of 0.5 to 1 mm depending on turbulence intensity. At flame radii of about 4 mm the expansion velocity is increasing to higher values. Because the effect of the laminar chemistry is domminant one cannot find an important influence of engine load during the flame kernel period. Reducing the contact areas between the flame kernel and the spark plug leads to a faster flame kernel development, which can be achieved by increasing the spark gap.

ACKNOWLEDGEMENTS

Support for this work was provided by Bundesministerium für Wirtschaft (Arbeitsgemeinschaft Industrieller Forschungsvereinigungen) contract AIF-Nr. 6359 comissioned by the Forschungsvereinigung Verbrennungskraftmaschinen (FVV). The authors would like to thank the members of the consulting group "Flame Kernel Formation" of the FVV for their cooperation within this research program.

REFERENCES

[1] L. Withrow and T.A. Boyd. *Ind. Eng. Chem.*, 23:539 -547, 1931.

[2] G.P. Beretta, M. Rashidi, and J.C. Keck. *Combustion and Flame*, 52:217–245, 1983.

[3] J.R. Smith. *SAE-Paper 820043*, 1982.

[4] E.G. Groff and J.F. Sinnamon. *SAE-Paper 821221*, 1982.

[5] W. Hentschel. In *VDI Berichte Nr. 617*, pages 347–367, 1986.

[6] M. Namazian, S. Hansen, E. Lyford-Pike, J.B. Sanchez-Barsse, J. Heywood, and J. Rife. *SAE-Paper 800044*, 1980.

[7] J. Bonini, L.Q. Xia, E. Chau, K. Hom, H.E. Stewart, R.F. Sawyer, and A.K. Oppenheim. *SAE Paper 870452*, 1987.

[8] G.F.W. Ziegler, A. Zettlitz, P. Meinhardt, R. Herweg, R. Maly, and W. Pfister. *SAE Paper 881634*, 1988.

[9] J. Chomiak. In *17th Symposium (Int) on Combustion*, pages 255–263. The Combustion Institute, 1979.

[10] Smith. J.R. *Flows in Internal Combustion Engines*, chapter The Influence of Turbulence on Flame Structure in an Engine., pages 67–73. Ed.: T. Uzkan, 1983.

[11] D. Bradley and F.K.K. Lung. *Combustustion and Flame*, 69:71–93, 1987.

[12] J.C. Keck, J.B. Heywood, and G. Noske. *SAE Paper 870164*, 1987.

[13] J.B. Tagalien, J.and Heywood. *Combustion and Flame*, 64:243–246, 1986.

[14] A.O. zur Loye and F.V. Bracco. *SAE-Paper 870454, Sp 715*, 1987.

[15] M.J. Hall, F.V. Bracco, and D.A. Santavicca. *SAE-Paper 860320*, 1986.

[16] J.A. Gatowski and J.B. Heywood. *SAE-Paper 852093*, 1985.

[17] J.C. Keck. In *19th Symposium (Int) on Combustion*, pages 1451–1466. The Combustion Institute, 1982.

[18] K.N.C. Bray. *Turbulent Flows with Premixed Reactants, Turbulent Reacting Flows. ,P.A. Libby and F.A. Williams (Eds.)*, pages 115–183. Springer, Berlin, 1980.

[19] G.G. DeSoete. In *13th Symp. (Int) on Combustion*, pages 735–743, 1971.

[20] Ö.L. Gülder. *SAE-Paper 841000*, 1984.

[21] P. Csallner. PhD thesis, TU München, Germany, 1981.

[22] G. DeSoete. In *First Specialists Meeting (International) of the Combustion Institut*, pages 49–54, 1981.

[23] S. Pischinger and J.B. Heywood. *SAE-Paper 880518*, 1988.

[24] D.R. Lancaster, R.B. Krieger, S.C. Sorensen, and W.L. Hull. *SAE- Paper 760160*, 1976.

[25] T.A. Baritaud. *SAE-Paper 872152*, 1987.

[26] R.G. Abdel-Gayed, D. Bradley, and M. Lawes. In *Proc. Roy. Soc. London Ser. A 414*, pages 389–413, 1987.